Chapter 2

Neural Stem Cell Fate Control on Micropatterned Substrates

Leonora Buzanska, Marzena Zychowicz, Ana Ruiz, and François Rossi

Abstract

Neural stem cell fate decisions are dependent upon signals coming from microenvironment composed of extracellular matrix proteins, soluble factors and specificity of cell–cell contacts. We have developed in vitro systems to trace developmental processes of neural stem cells and to control their fate commitment. Applied technologies include nano/micro-fabrication techniques, like microcontact printing and piezoelectric microspotting of biomolecules on plasma deposited cell repellent surface. Designed bioactive domains with controlled content and geometry served as a template to immobilize neural stem cells to the surface and direct their differentiation. Migration and axon-like outgrowth have been successfully guided by means of interconnected squares configuration. Receptor mediated versus electrostatic interactions on the cell membrane–surface interface were crucial to keep the cells either in neurally committed or in non-differentiated stages by fibronectin or poly-L-lysine pattern, respectively. Single cell versus multicellular positioning further promoted stem cells non-differentiated stage. Activation of intracellular pathways by signaling molecules (Wnt, CNTF, Jagged, Notch and DKK-1) microspotted with fibronectin directed differentiation into astrocytic and neuronal lineages, as revealed by immunocytochemical and molecular analysis. Our results proved that neural stem cell fate decisions can be influenced by manipulating the composition and architecture of the 2D bioactive domains reflecting their natural niche microenvironment.

Key words Neural stem cells, Piezoelectric microspotting, Microcontact printing, Bioactive domains

1 Introduction

Human neural stem cells are widely investigated due to their promise held for the therapy of neurological disorders. Their specific properties to incorporate in vivo into the damaged neuronal tissue and differentiate into specific neural cell types, favor the opinion of their possible replacement rather than adjuvant features, as compared to mesenchymal stem cells. Thus, it is important to set up optimized in vitro microenvironments mimicking in vivo conditions and enabling to control human Neural Stem Cells (hNSC) fate commitment and differentiation. Standardized conditions for in vitro culture and fate commitment of therapeutically competent hNSC are, although widely studied, not thor-

Amit K. Srivastava et al. (eds.), *Stem Cell Technologies in Neuroscience*, Neuromethods, vol. 126,
DOI 10.1007/978-1-4939-7024-7_2,

oughly characterized. Biotechnological innovations provide tools, such as advanced stem cell culture protocols and generation of new, tunable biomaterials capable of releasing specific signals in a spatially and temporally controlled manner. These innovations together with emerging technologies of fabrication of 2D and 3D cell culture platforms provide opportunities to create in vitro nature-like conditions for stem cell-based systems. Such in vitro systems are referred to, in the literature, as "biomimetic" due to their ability to mimic in vivo native microenvironments [1, 2]. To adequately mimic in vivo neural stem cell niche, in vitro one should learn from the experience and knowledge of in vivo systems. The fate of neural stem cells is controlled by a number of signaling cues present in the stem cell niche. In addition to structural elements like extracellular matrix (ECM) proteins, proteoglycans and other cells, microenvironment of the niche also include soluble factors, such as cytokines, growth factors, cell adhesion molecules, hormones, and neurotransmitters. Complex mutually time- and space-dependent cell–cell and cell–ECM protein/proteoglycan interactions have been shown to play an essential role in cell fate decisions [3, 4]. These interactions may influence the binding of soluble signaling molecules to cellular receptors and may change their expression [5]. On the other hand, the presence of signaling proteins that bind to their specific receptors, direct cell developmental decisions whether to proliferate and maintain their stemness, or to induce neural differentiation [6]. In vitro culture platforms including structural and soluble elements typical for NSC microenvironments have been proposed to investigate the influence of physical cues of NSC fate decisions, but also to define molecular mechanisms underlying these decisions. Variety of tested physical cues comprised geometry of 2D micropatterns [7–11], substrate stiffness [12, 13], topography of the surface [4, 10] and gradients of substrates in microfluidic systems [14, 15]. Directed differentiation of stem cells by changing nanoscale topography of the adhesive substrates has been linked to the modulated genomic expression and the presence of so called "contact guidance spots" in the cell membrane [16]. Further, the surface-printed microdot array in nanoscale was proposed for controlling axon branch formation [17]. Changing geometry of the pattern of microprinted fibronectin and poly-L-lysine biofunctional domains applied in our experiments reinforced directed neuronal differentiation and axonal outgrowth of Human Umbilical Cord Blood derived Neural Stem Cells (HUCB-NSC) [9, 18]. In addition to cell/microenvironment structural interactions, microengineering techniques were used to trace specific, receptor mediated cellular responses to soluble cues. Independent research groups, including our laboratory, have shown that signaling molecules immobilized to the surface together with ECM proteins influence human neural stem cells fate decisions. Soen et al. [19] using ECM

proteins combined with different signaling molecules, applied a combinatory approach for human NSC lineage commitment and successfully directed their differentiation. In our studies, defined signaling molecules (CNTF, Notch, Jagged, Wnt3a, Shh, Dkk-1, BMP4), each spotted as a single domain in repetition with the ECM protein (fibronectin), provided specific cues to fate commitment of HUCB-NSC, either stemness maintenance or differentiation into neuronal or astrocytic lineages [8].

In this report, we introduce bioengineering strategies to build up microenvironments at microscale, for the effective fate control of neural stem cells derived from human cord blood. The single or multi cell microarrays are good alternative for the standard culture systems where cell response to a different adhesive materials and/or bioactive compound is investigated. Moreover, micropatterning provides the conditions where exactly the same culture settings (cell density, medium composition, temperature, humidity, and oxygen concentration) can be obtained within the same culture dish. The bioactive microdomains on cell culture platforms are fabricated using either soft-lithographic technique—microcontact printing or piezoelectric spotting, the latter technique enabling deposition of different microdroplets with defined substrate content.

2 Materials

2.1 Neural Stem Cell Culture

Since the availability of human neural stem cells is very limited, we have established an untransformed cell line that is derived from human umbilical cord blood non-hematopoietic mononuclear cells, which were maintained and selected in the presence of 10% FBS and EGF. These cells, named Human Umbilical Cord Blood Neural Stem Cells (HUCB-NSCs) have molecular and functional properties of neural stem cells: they are clonogenic, and after differentiation give rise to three types of cells: neurons, astrocytes and oligodendroglial cells. This cell line has two population of growth: when cultured in serum free conditions cells are free floating, exhibit undifferentiated state of NSC while when they are grown in the presence of 2% serum and ITS supplement (insulin, transferrin, selenium) cells start to adhere and spontaneously differentiate, exhibiting the neuronal (β-tub III, Map-2, NF200) or glial (GFAP, S100β, NG2) markers [20].

For the purpose of the described experiments cells were maintained in serum free medium (DMEM/F12, B27 1:50, EGF 20 ng/mL, AAS) or low serum medium (DMEM/F12, 2% FBS, ITS, AAS). Cells were passaged once a week at 1:4 ratio and maintained at 37 °C, 5% CO_2, and 95% humidity.

2.2 Cell Culture Platforms with Functional Domains Biopatterned by Microcontact Printing and Microspotting

2.2.1 Substrate Preparation by Plasma Polymerization

Plasma polymerization allows depositing conformal thin polymeric films that can either promote or prevent cell adhesion, depending on the polymer chemical function. Plasma polymers are deposited using a glow discharge created from monomer vapor by using capacitive coupled plasma sources. The glow discharge is generated by a high frequency electric field applied between two parallel plate electrodes and contains ions, free electrons and monomer fragments. The properties of the films can be controlled by tuning the discharge parameters, particularly pressure, gas residence time and power.

Cell repellent polyethylene oxide (PEO) has been used as substrate for protein and cell patterning. The PEO films have been deposited by plasma-enhanced chemical vapor deposition in a capacitive coupled reactor, using a glow discharge in diethylene glycol dimethyl ether vapor (Sigma-Aldrich). The plasma reactor had a vessel size of 300 × 300 × 150 mm and two symmetric internal parallel-plate electrodes of 140 mm diameter separated a distance of 50 mm. The plasma was generated by a radio frequency generator operating at 13.56 MHz and connected to the upper electrode, whereas the bottom electrode was grounded and used as sample holder. A 20 mm -thick PEO-like layer was deposited using a pulsed plasma discharge (time on = 10 ms, time off = 100 ms, nominal power = 2 W) of pure diethylene glycol dimethyl ether vapors and a constant working pressure of 20 mTorr. For SPR imaging analysis, the film deposited on the SPR slide was thinner than 20 nm in order to remain in the thickness range usable by the instrument. Ellipsometry measurements of the same PEO-like film deposited on silicon gave a film thickness of 11.5 nm [21].

Previous studies [22] have demonstrated that pulsed plasma polymerization of pure diethylene glycol dimethyl ether monomer allowed the fabrication of stable thin layers with a high retention of polyethylene oxide character and a strong anti-fouling character. Such films could even be microstructured with other polymer functionalities by using photolithographic processes without altering their surface properties [23].

For microspotting, the films were deposited on optical glass slides sonicated successively in trichloroethane, acetone, and ethanol, 5 min each time, and finally rinsed in ultrapure Millipore water and dried under a N_2 flow. In the case of microcontact printing, the PEO-like layer was deposited directly at the bottom of sterile petri dishes rinsed in pure water.

2.2.2 Microcontact Printing (MCP) on PEO-Like Films

Master Fabrication

The first step of the microcontact printing process is the creation of masters having the geometries of interest to reproduce. Photolithography and plasma etching techniques were used to fabricate silicon masters with depth features of 2.5 μm. A positive photoresist (Microposit S1813, Shipley) was spin coated at 900 rpm for 13 s and 2000 rpm for 1 min on silicon and pre-baked (110 °C, 2 min). The resist was then exposed to a laser beam (λ = 405 nm)

through ink-printed slides masks. The exposed photoresist was then developed by immersing the slides in Microposit MF-321 developer (Shipley) for 45 s. The samples were washed thoroughly in water and post baked again at 110 °C for 2 min. The patterns created in the photoresist were transferred to the silicon underneath by reactive ion etching. The pattern transfer was done in a inductively coupled plasma equipment introducing SF_6 gas as reagent. The pressure in the reactor chamber was 10 mTorr, the power was set to 400 W and the bias voltage to −60 V. After plasma etching, the photoresist was dissolved by ultrasonicating the slides in acetone for 1 min. In order to avoid adhesion of the stamp to the master and make the peel-off easier during the replica molding step, the silicon masters were coated with a Teflon-like layer, CFx, deposited by plasma polymerization from C_4F_8 gas at 50 mTorr and −40 V of bias. The presence of the low adhesion teflon-like layer was crucial to achieving a good, undamaged replica of the microstructures by facilitating the PDMS peel off.

Replica Molding

The rubber stamps were fabricated by casting the silicon master in polydimethylsiloxane (PDMS). A mixture of polymer precursors was done vigorously stirring 1:10 parts of prepolymer and curing agent (Sylgard 184). The viscous mixture was poured on the masters, left to degas at room temperature for 1 h and cured at 65 °C for 4 h.

Direct Printing of Biomolecules

The microstructured PDMS stamps, fabricated by casting the silicon masters produced by photolithography, have been used for the direct printing of several biomolecules onto plasma polymerized PEO-like films. The PDMS stamps were ultrasonicated in ethanol for 5 min and cleaned in soft O_2 plasma (200 W, 1.2 mTorr) for 30 s in order to increase the hydrophilic character of the PDMS by forming more silica groups on the surface. The hydrophilic PDMS stamps were then inked at room temperature with the biomolecule solution. Proteins, such as BSA, poly-L-lysine, (PLL) and fibronectin (FN), as well as protein antibodies can be successfully printed [24]. Of particular interest for HUCB-NSC fate control were the PLL and FN patterns. For microcontact printing, FITC-labeled PLL was diluted in carbonate buffer (100 mM) at 25 μg/mL and pH 8.4, while FN from human plasma (Sigma, F0895) was used at concentrations of 42 μg/mL and 167 μg/mL diluted in printing buffer (100 mM acetate (Riedel deHaën), pH 5, 5 mM EDTA (Merck), 0.01% Triton X-100 (Fluka), and 0.1% glycerol (Carlo Erba). Figure 1 shows fluorescence microscopy pictures of PLL patterns, evidencing those different geometries, i.e., size, shape, and separation of PLL domains, can be obtained by tailoring the stamp motifs. PLL patterns at highest resolution (one cell, 10 μm) are also shown. Fluorescent imaging of proteins was carried out in a Zeiss inverted microscope Axiovert 200. The inking time was varied according to the biomolecule to adsorb. PLL was incubated

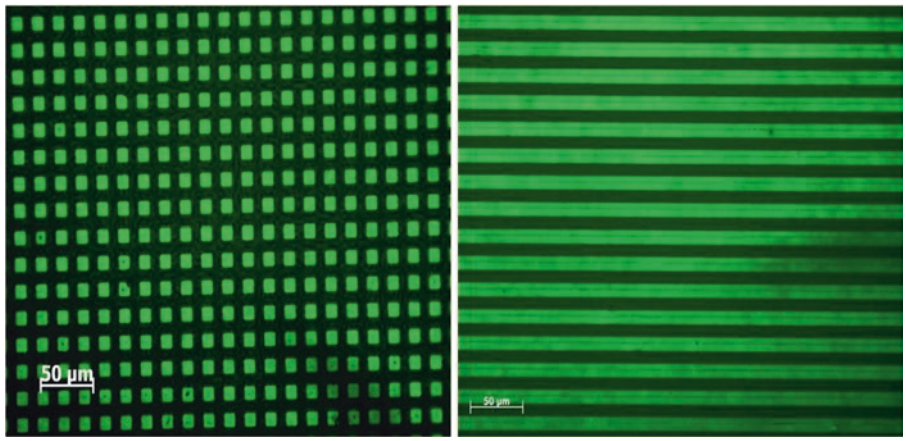

Fig. 1 Fluorescence microscopy images of poly-L-lysine (FITC PLL in *green*) patterns on plasma PEO-like surfaces. The PLL patterns are 10 × 10 µm, *squares* and 10 µm *wide lines*, which commensurate with cell size

for 15 min while fibronectin needed 45 min of incubation to be adsorbed to PDMS. Then, the excess of protein solution was removed; the stamps were dried in a N_2 stream and then put in conformal contact with the PEO-like coated substrates. The PDMS stamp was lifted off vertically and the samples were rinsed with the buffer solution and dried in a nitrogen stream. Before seeding the cells, the patterned substrates were UV sterilized for 15 min. Using this method, the biomolecules attached to the PDMS can transfer and remain adhering to the substrate [7, 21].

2.2.3 Microspotting on PEO-Like Films

In order to obtain the custom dependent array of different molecules on the same platform we have used the microspotting technology. This allows placing the desired biomolecules in designed manner, which means the size of domains, the layout of array, different compositions and concentrations of spotted solution, spatial distribution of domains on the cultured surface, precise volume of spotted solution, making a very reproducible array. This technology, as almost all micropatterning techniques, requires the cell-repellent surface to be deposited on the culture area in order to achieve the fouling/non-fouling contrast. One method to create such non-fouling surface is to deposit a polyethylene oxide-like, PEO-like film, by plasma polymerization [25, 26]. It is a fast method and can be operated on plastic, glass, also within the chambers or standard culture vessels (petri dish) [25]. Moreover, when the PEO-like surface is dry it provides very good immobilization of microspotted proteins.

Spotting of the proteins on the substrates was performed in a S3 sciFLEXARRAYER (Scienion AG, Germany) piezoelectric dispenser. The instrument has a three axis micro-positioning system (accuracy 10 mm) and is equipped with a glass nozzle 80 µm in diameter. A stroboscopic camera allows visual monitoring to adjust

piezo voltages and pulse durations for reliable droplet ejection and to avoid satellite drops. Single drops ejected from the nozzle have a volume of 400 pl. Between 1- and 5-drop volumes were dispensed to obtain surface domains of different sizes. The vertical separation between the nozzle and the substrate was typically 0.5 mm. The distance between spots can vary but typically for cell culture experiments a pitch of 600 μm was used. Four-drop volume spots and a pitch of 600 μm have been chosen to prepare microarrays of different biomolecules. They included fibronectin, laminin, collagen I, collagen III, collagen V, bovine serum albumin (BSA), and poly-L-lysine. Finally, fibronectin was chosen as optimal for HUCB-NSC adhesion and arrays of 10 × 10 spots arranged in two lines of three arrays each were prepared on half slides using FN diluted in printing buffer at concentrations of 21, 42, 84, 167, and 333 μg/mL.

3 Methods

3.1 Functional Analysis of Microprinted and Microspotted Domains

3.1.1 ToF–SIMS Mapping of Biomolecules Patterned on PEO-Like Films by MCP

Time of flight—secondary ion mass spectrometry (ToF–SIMS) was used to characterize the protein or polypeptide patterns. ToF–SIMS was done in a TOF-IV spectrometer (ION TOF GmbH, Germany). Figure 2 depicts ToF–SIMS analyses of fibronectin on PEO-like films. The CH_3O mass in the central image of the figure is ascribed to the polyethylene oxide, whereas C–N mass forming bright squares in the right image belongs to the protein. The protein patterns exhibited a firm stability when put in solution, as confirmed by ToF–SIMS analyses evidencing the presence of well-defined impressions after 24 h in water.

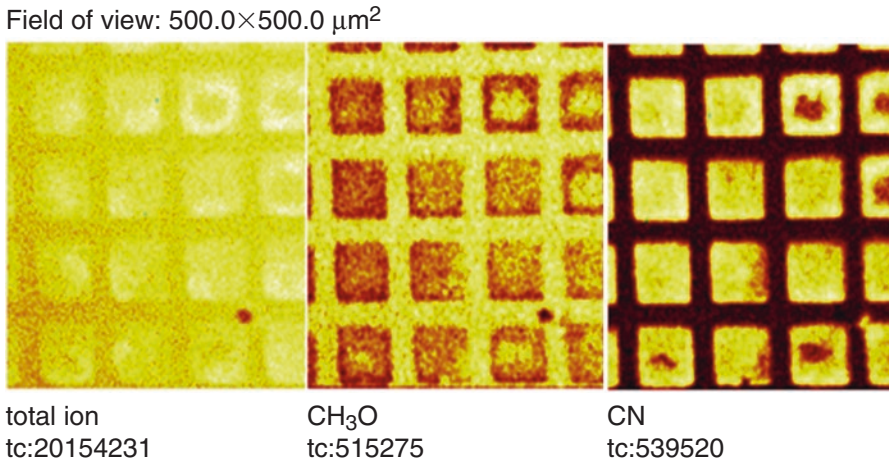

Fig. 2 ToF–SIMS mapping of Fibronectin patterned on PEO-like films by MCP

3.1.2 Ellipsometry of Functional Domains

The methodology of ellipsometry analysis has been described in detail in (Ceriotti et al 2007, Ruiz 2013). Ellipsometric data were acquired with a variable angle imaging ellipsometer (model EP3 by Nanofilm Surface Analysis GmbH, Germany) and present as the thickness map of the biomolecule. All imaging measurements were performed in air at room temperature at an angle of incidence of 42°, using a monochromatized high power Xe lamp at a wavelength of $\lambda = 554.3$ nm. A polarizer-compensator sample- analyzer (PCSA) null-ellipsometric procedure was used to obtain maps of the Δ and Ψ angles for the selected area. Thickness maps were calculated from the Δ and Ψ maps by point-by-point modeling with the software EP3View provided with the ellipsometer, using a two-layer model with PEO as first layer and the stamped FN as the second. The thickness (11.5 nm) and the refractive index of plasma deposited PEO (nPEO = 1.52) were independently determined by an angle-resolved measurement. A refractive index of 1.46 was used for both FN and PLL [7, 27]. Ellipsometric data were acquired with a variable angle imaging ellipsometer and present as the thickness map of the biomolecule. We have shown equal distribution of protein deposited by MCP (Figs. 3 and 4), and for fibronectin microspotted at different protein concentration, (Fig. 5).

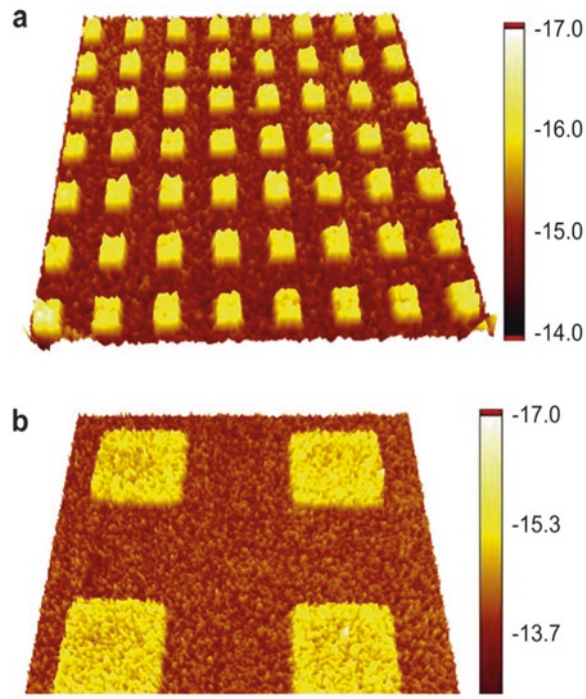

Fig. 3 Thickness maps of PLL stamped on plasma-deposited PEO-like at pH 7, after rinsing, calculated from ellipsometric D- and J-maps. The thickness is given in nm with respect to the Si surface. Size of the maps: (**a**) 1500 mm, 1690 mm and (**b**) 380 mm, 390 mm. Adapted from [7]

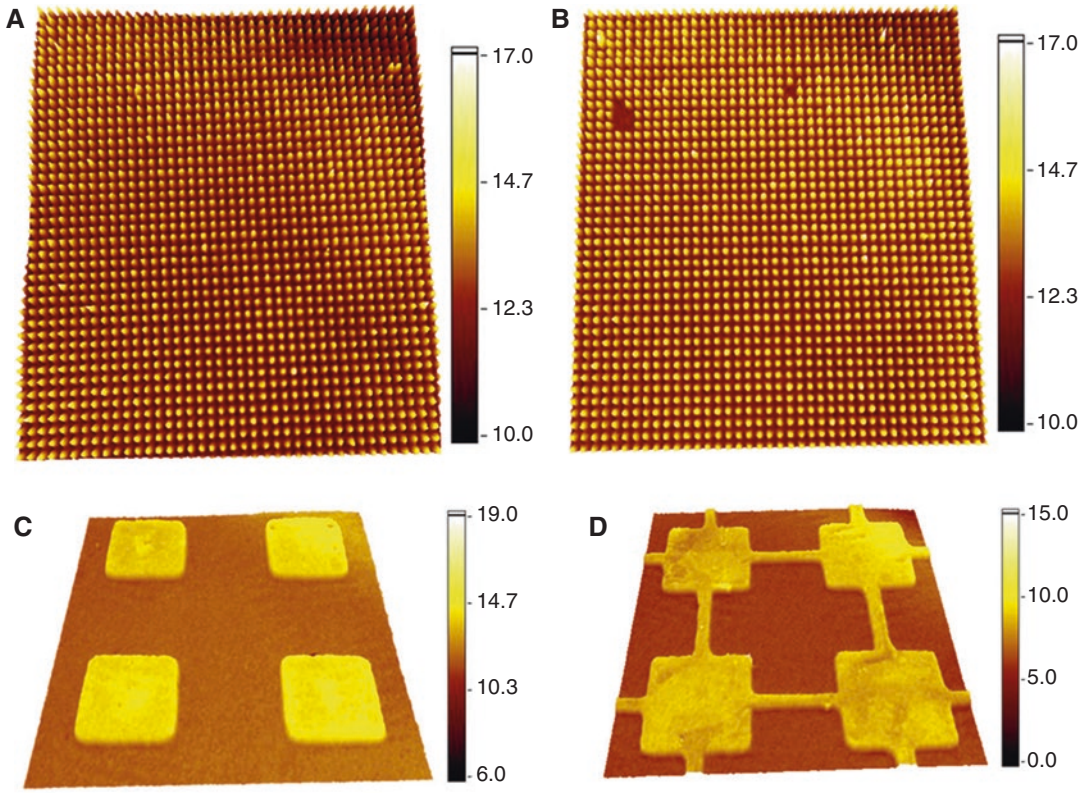

Fig. 4 3D thickness maps of 5 μm *square* MCP patterns of FN 42 μg/mL (**a**) and FN 167 μg/mL (**b**), as well as of 120 μm *square patterns* of FN 42 μg/mL without (**c**) and with (**d**) *interconnecting lines*. The thickness is calculated from ellipsometric Δ- and Ψ-maps and given in nm with respect to the Si surface. Size of the maps: 400 × 400 μm. Adapted from [7]

The amount of FN that remained on the PEO surface after rinsing (Fig. 5b) saturates at 112 ng/cm^2. Using a nominal FN concentration of 84 μg/mL resulted in a retention on PEO close to the saturation value (row 2 and 3 on Fig. 5); thus, the FN concentration of 84 μg/mL was chosen for further spotting experiments.

3.1.3 Surface Plasmon Resonance (SPR) of Biofunctional Domains

Biological functionality of the bioengineered surfaces was characterized by Surface Plasmon Resonance (SPR) to show protein spot reactivity. SPR enabled verification on fibronectin domains of accessibility of the fibronectin receptor binding sites for cell integrin receptors as estimated by binding of anti RGD antibody (Fig. 6).

The reaction of anti-fibronectin monoclonal antibody RGD-specific (Ab-RGD) on spots of six different fibronectin concentrations was tested. We have shown dependence of reactivity of antibody binding through RGD domain upon deposited protein concentration: the reaction was significant starting from the concentration of 42 μg/mL of spotted fibronectin. The control reactions with BSA and anti-ovalbumin were negative (Fig. 6). Thus we confirmed the accessibility of the protein for cell integrin receptor binding.

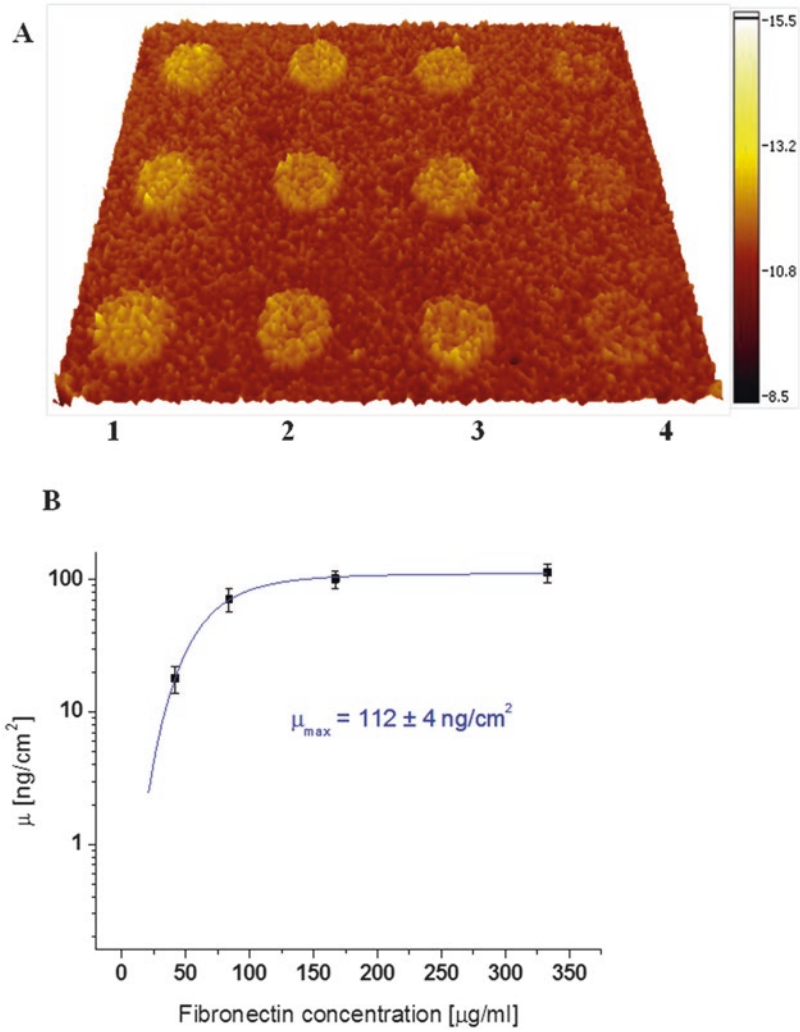

Fig. 5 (**a**) Thickness maps of Fn spots on plasma-deposited PEO-like film after rinsing in water and calculated from ellipsometric D and J maps. The thickness is given in nm with respect to the Si surface and includes the PEO-like layer (11.5 nm). Fibronectin concentration = 167 μg/mL (column 1), 84 μg/mL (columns 2 and 3), and 42 μg/mL (column 4). Size of the maps: 2000–1400 μm. (**b**) Mass density (m) of the fibronectin spots after rinsing as a function of the protein concentration in the spotted solution. It was averaged over six equivalent spots deposited from a solution with equal protein concentration. Adapted from [25]

3.2 Neural Stem Cell Patterning on Microprinted Arrays

Diverse geometry and resolution of the microcontact printed domains can be obtained to accommodate either single cells (pattern size of 10–20 μm) or groups of cells (pattern sizes typically above 100 μm) (Fig. 7). Such arrays were used to study different developmental processes of HUCB-NSC and their responses to the external stimuli. Designed bioactive domains with controlled biomaterial content and geometry served as a template to immobilize neural stem cells to the surface. HUCB-NSC readily adhered to bioactive surface of both: poly-L-lysine and fibronectin domains and presented good confinement to the domains through the 21 days of experiment.

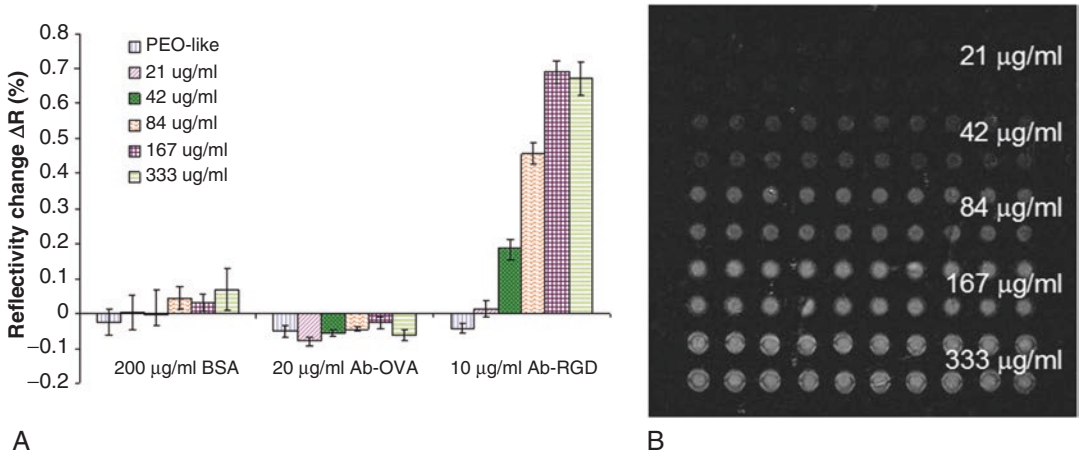

Fig. 6 (**a**) Reflectivity change due to the injection of 200 mg/mL BSA, 20 μg/mL anti-ovalbumin (Ab-OVA) and 10 μg/mL mouse anti-fibronectin monoclonal antibody RGD-specific (Ab-RGD) on spots of different fibronectin concentrations. (**b**) SPR difference image of the fibronectin array after the interaction with the 10 mg/mL Ab-RGD. Adapted from [25]

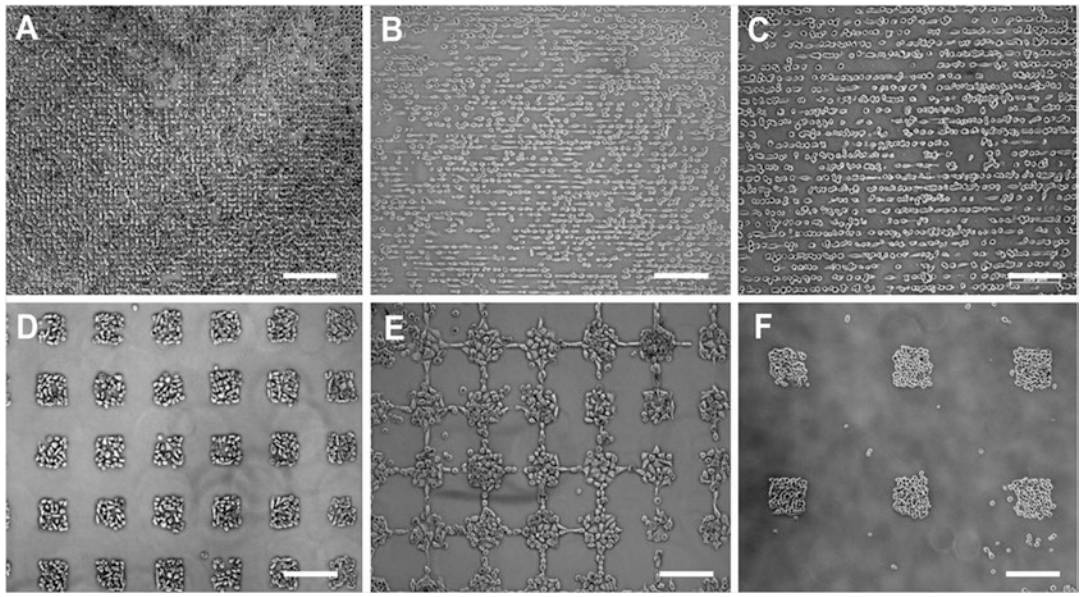

Fig. 7 Patterns of HUCB-NSC grown on PLL: 10 μm posts (**a**), 10 μm-width *lines* (**b**), 20 μm *lines* (**c**), 120 μm *squares* (**d**), 120 μm *squares* and *interconnecting lines* (**e**), and 150 μm *squares* with long distance (**f**), scale bar 200 μm. Adapted from [8]

When using microcontact printing to produce poly-L-lysine and fibronectin patterns of length-scales that commensurate with cell size, single stem cells arrays were achieved and the stem cells were constrained to redistribute their cytoplasm in the permitted areas. Figure 8 shows stem cells patterns on PLL and FN bioactive areas of 10 μm lateral dimensions, either squares or lines, separated by 10 μm cell-repellent gap. While single cell arrays of spherical HUCB-NSC were achieved on the square patterns, the

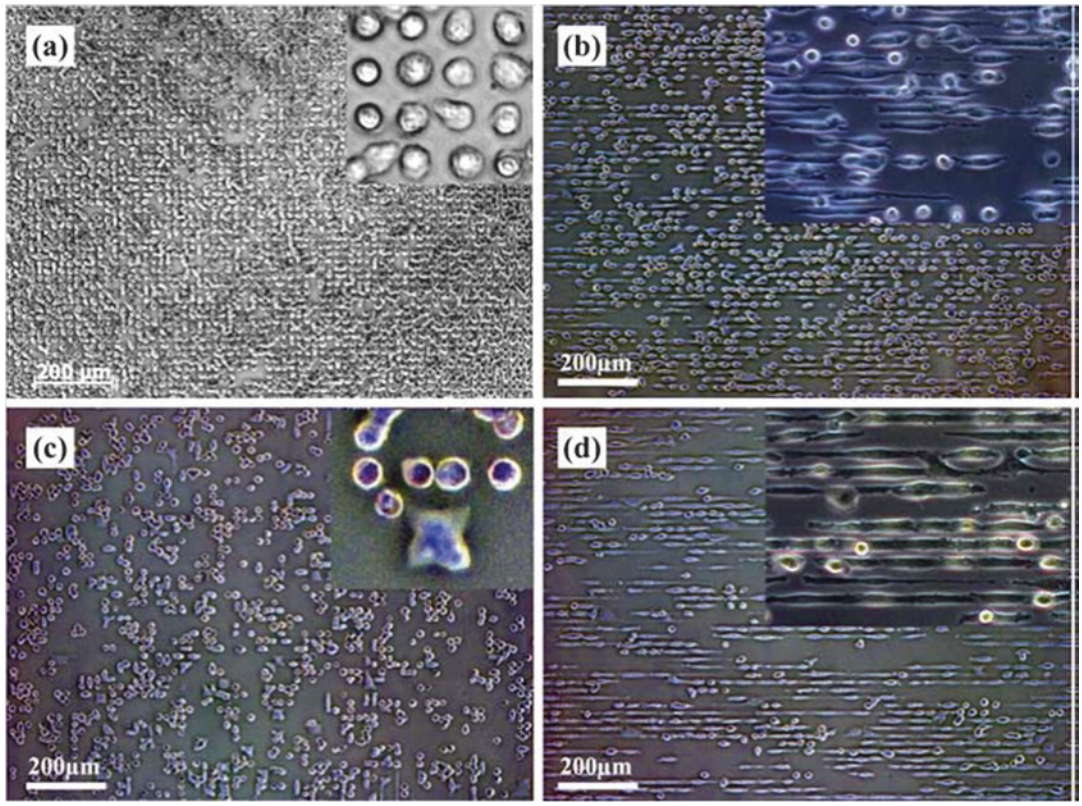

Fig. 8 Phase-contrast images recorded on live cells of HUCB-NSC after 1 day culturing on PLL (**a**, **b**) and fibronectin (**c**, **d**) patterns of 10 × 10 μm *dots* (a, c) and10 μm *wide lines* (**b**, **d**). Adapted from [28]

cells stretched and elongated along the line patterns. The extent of elongation was higher on the FN line pattern (Fig. 8d) than on the PLL one (Fig. 8b), evidencing the dependence of the phenotype on the mode of cell attachment (specific, integrin-mediated versus nonspecific, electrostatic cell binding) [28]. The larger aspect-ratio of the cells grown on fibronectin lines is in agreement with other observations of higher rate of spreading of HUCB-NSC on printed fibronectin as compared to PLL [26]. This is also confirmed by HUCB-NSC scanning electron microscopy images of cells plated either on PLL (Fig. 9a) or on fibronectin (Fig. 9b).

HUCB-NSC attach weakly to PLL through anionic–cationic interactions. The low cell spreading on PLL, together with the background passivation by plasma-PEO, enable obtaining high-density arrays of individual cells, as observed in Fig. 8a. DAPI staining revealed that the nuclei of the cells attached to the 10 μm wide PLL squares occupy all the adhesive PLL area, thus the cells are constrained to maintain a spherical shape. As previously mentioned, cell adhesion to fibronectin involves integrin and focal

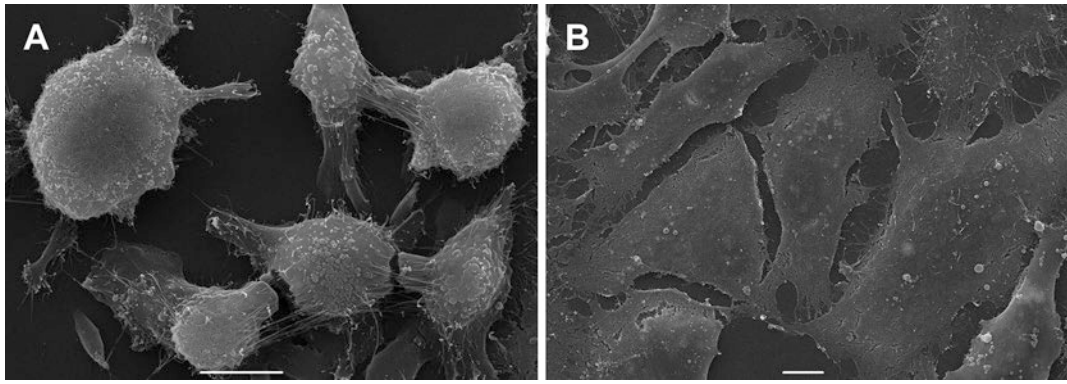

Fig. 9 Scanning electron microscopy images of HUCB-NSC cells plated on poly-L-lysine (**a**) and fibronectin (**b**). Note the flattened phenotype of fibronectin attached cells in in the presence of serum. Scale bar: 10 μm. Adapted and modified from [9]

adhesion signaling, which allows advanced cell spreading [29]. The cell packing observed on the fibronectin 10 μm squares (Fig. 8c) is limited by adhesion/spreading competition. Upon attachment, the cells readily spread which allows an adherent cell to invade neighboring, free fibronectin squares, as shown in the magnified image in the inset of Fig. 8c, where one cell occupies four neighboring fibronectin squares.

3.3 Neural Stem Cell Patterning on Microspotted Arrays

Firstly, we were interested in selecting the best ECM protein and its optimal concentration in term of cell adhesion and quality of samples during all the workflow of cell culturing procedure (cell seeding, medium changing, fixation) and collecting the data (staining and immunofluorescence). We have tested three (21, 42, and 84 μg/mL) concentrations of proteins: fibronectin, laminin, and collagen IV, which are the ECM proteins found in the neural stem cell niche in the brain. After cell seeding in the $5 \times 10^4/cm^2$ cell density and the 24 h of culture in the medium containing 2% of FBS, the best adhesion and optimal cell growth was observed on fibronectin, even in the lowest protein concentration. The optimal domain stability during the several day culture and sustaining/not promoting of advanced directed neuronal or glial differentiation enables to use the fibronectin as a reference protein for further analysis of influence of signaling proteins on HUCB-NSC fate decisions (Fig. 10a) [25].

The following step was to optimize the spotting protocol for the fabrication of ECM protein microarrays with fibronectin for HUCB-NSC cell attachment in terms of spot size and array layout using fibronectin as protein model [25].

The concentration of 84 μg/mL of fibronectin and the spot size of 4 microspotted drops were chosen for experiments with neural stem cells (Fig. 11).

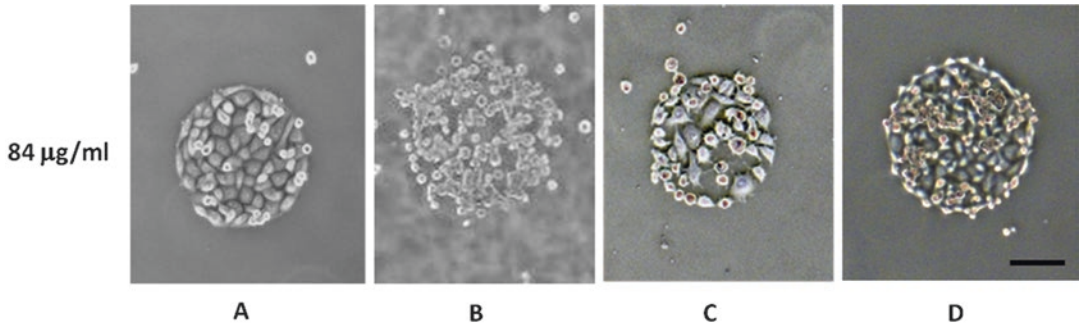

Fig. 10 HUCB-NSCs on fibronectin (**a**), laminin (**b**), collagen V (**c**), and vitronectin (**d**) after 4 days of culture on 3-drop protein spots. The effect of different protein types is visible. Fifty thousands of cells were seeded and maintained in standard culture conditions in presence of 2% serum. The scale bar is 100 µm. Adapted and modified from [25]

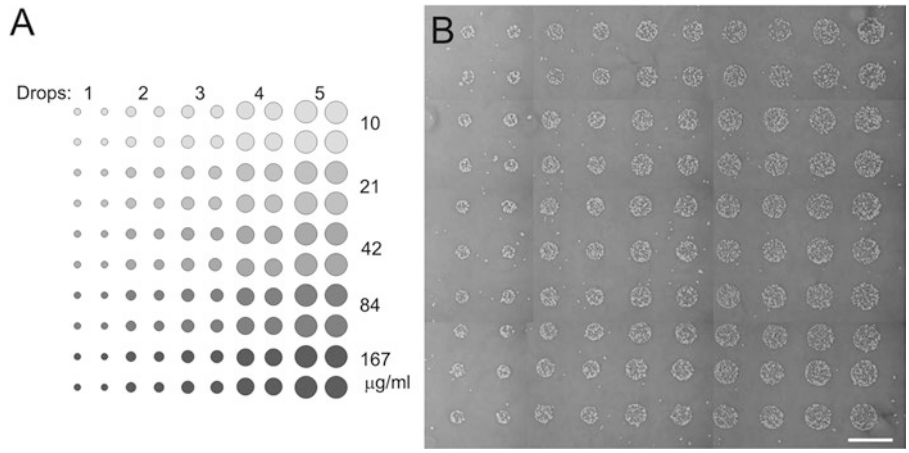

Fig. 11 The spots of fibronectin array were obtained by dispensing different number of drops (from *left*: 1–5 drops, two columns for each drop number) and fibronectin concentrations (from *top*: 10, 21, 42, 84, 167 µg/mL, two rows for each concentration) (**A**). HUCB-NSCs adhesion to the array (10 × 10) of fibronectin spots on PEO-coated slides, after 1 day of cell culture (**B**). Adapted from [8]

3.4 Neural Stem Cell Fate Control on Microprinted Arrays

Microarray layouts of different geometries and biomolecules were prepared to control stem cell adhesion and differentiation. Fate decision of the HUCB-NSC was controlled by the composition and geometry of the active domains. While electrostatic interaction of the cells with the poly-L-lysine kept them non-differentiated, specific integrin receptor -driven interaction with fibronectin, stimulated neuronal differentiation. This was further enhanced by the serum withdraw in the presence of the neuromorphogene—dBcAMP and the specific geometry of the domain—interconnected lines directed neuronal outgrowth.

3.4.1 Proliferation and Migration of NSC on Microprinted Patterns

To estimate the effect of different species of bioprinted domains on proliferation of HUCB-NSC, cells were cultured on the surface patterned with FN or PLL (Fig. 12). Such pattern enables to capture cells on the defined squares of 100 µm side with a 100 µm gap between the squares.

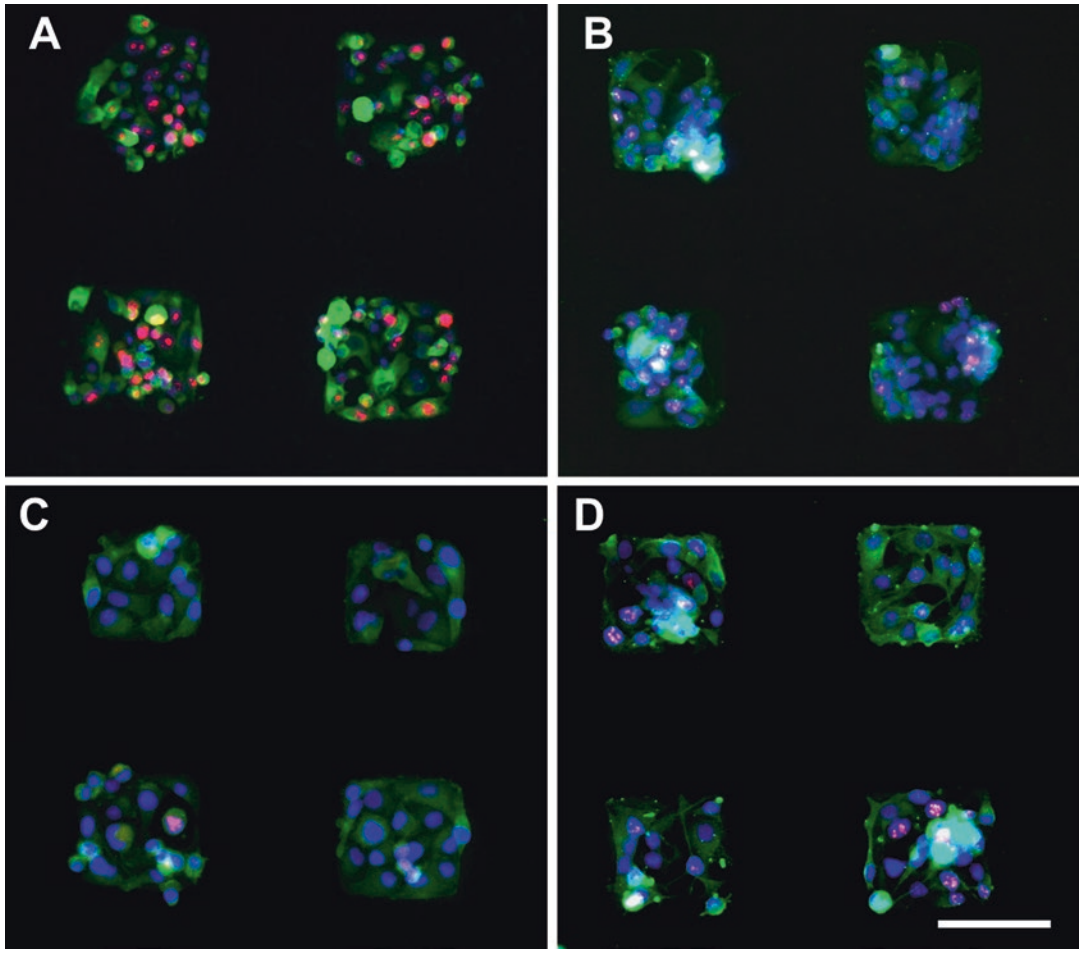

Fig. 12 Immunofluorescence images of HUCB-NSC cells plated on either poly-L-lysine (**a**, **b**) or fibronectin (**c**, **d**) patterns at 2.5×10^4 cells/cm^2 plating density in 2% of serum (**a**, **c**) and serum free (**b**, **d**) medium at day 4. Cells grown on poly-L-lysine show higher proliferation rate (Ki-67-positive *red dots* in *blue* stained nuclei) than on fibronectin. The β-III tubulin-positive cells are presented in *green*. Cell nuclei are contra-stained with Hoechst (*blue*). Scale bar: 100 μm. Adapted from [9]

The proliferation assay was performed at different seeding density and in the serum free and low serum culture medium [9]. We have measured the percentage of proliferating (Ki67 positive HUCB-NSC) cells per deposited microdomain. We reported that the proliferation rate was higher on poly-L-lysine than on fibronectin printed domains, and poly-L-lysine was able to immobilize more cells on square domains at the same size (Fig. 12). Moreover, the PLL domains, especially in serum free medium, kept the cells at round morphology in a proliferating, non-differentiating state while fibronectin domains of the same size allowed appearance of flattened, strongly attached cells, displaying long protrusions and outgrowth, and revealing lower proliferation rate than on poly-L-lysine, however still at the level even up to 60% of Ki67

positive cells. The ECM protein also promoted neural differentiation of HUCB-NSC cultured on microcontact printed biofunctional arrays [9]. To test whether the deposited biomolecules are able to influence the migration capacity of HUCB-NSC we have performed 24-h observation of HUCB-NSC migrating on micropatterned squares with interconnecting lines printed with either pol-L-lysine or fibronectin. We found that electrostatic type of adhesion is less intensive/strong allowing for cell movement from one domain to another, while ECM protein keeps the cells in the place not allowing for long distance migration [7].

3.4.2 Differentiation of NSC on Microprinted Patterns of Different Size and Biomolecule

Microarray layouts of different geometries (lines and posts) and biomolecules (PLL and FN) were prepared to control stem cell adhesion and differentiation. The layout of one cell resolution posts and lines of PLL and FN revealed that PLL accommodates non-differentiated cells, while FN promotes spreading and neural differentiation. Nestin immunostaining of HUCB-NSC on PLL 10 μm posts (Fig. 13a) and lines (Fig. 13b) confirmed that observation. PLL functionalization was useful for keeping the cells in nestin positive, non-differentiated state (Fig. 13), while the cells grown on fibronectin were negative for nestin immunostaining, indicating that they are at early stages of neuronal or astrocytic differentiation (not shown). Well-defined one-cell resolution patterns of cells with spherical morphology were identified on PLL 10 × 10 μm squares (Fig. 8a). Together with the positive results for nestin staining (Fig. 13), this indicates that PLL one-cell resolution pattern retained the most homogeneous non-differentiated stem cell populations. On PLL patterns of 10 μm wide lines most of the cells were in range of 10–40 μm, while fibronectin patterns accommo-

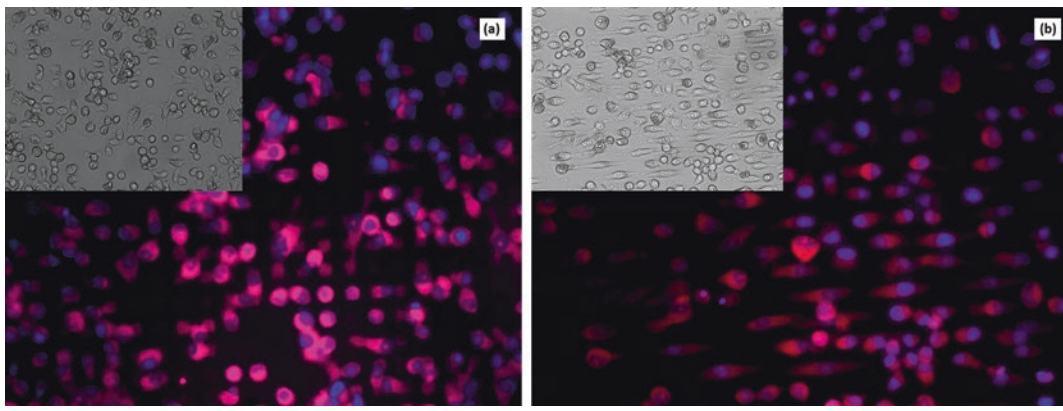

Fig. 13 Fluorescence microscopy images of nestin immunostaining (*red*) of HUCB-NSC after 7 days culturing on PLL *squares* (**a**) and *lines* (**b**). Insets show the corresponding bright field images. Cell nuclei (*blue*) are stained with Hoechst 33342. Adapted and modified from [28]

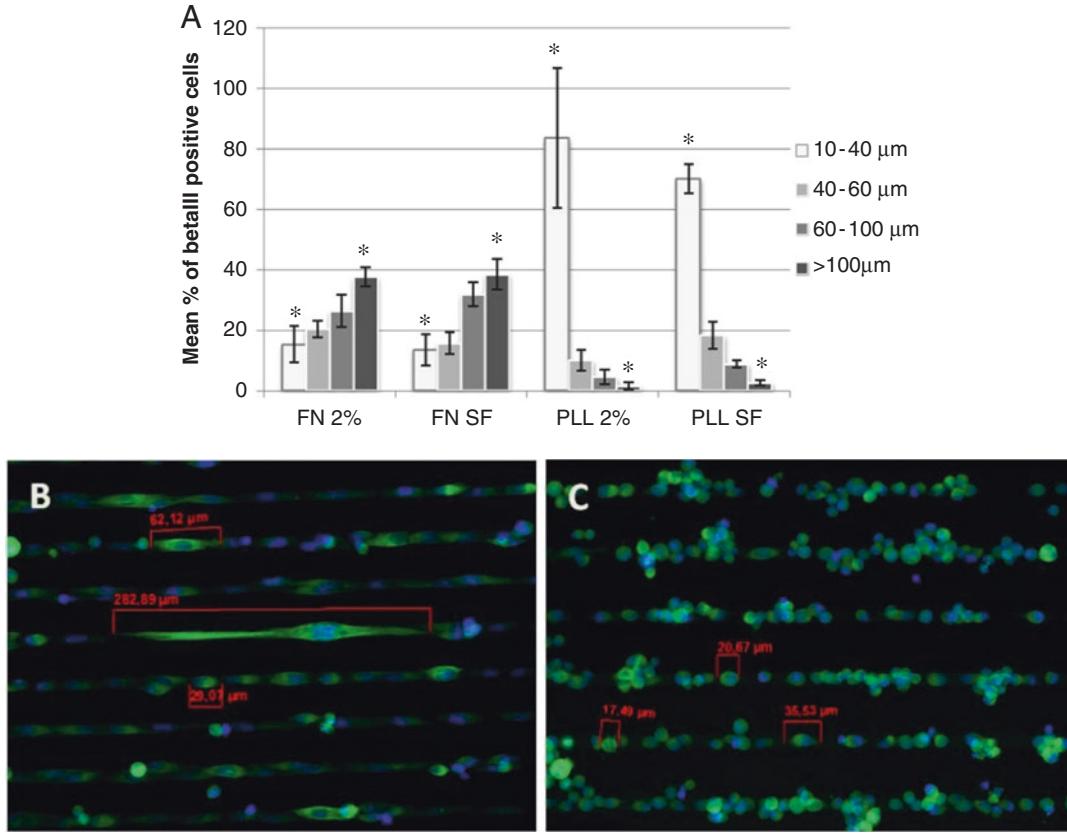

Fig. 14 Distribution of β-tubulin III-positive cells with different cell length parameters, after 24 h of culture (**a**). Immunostaining of β-tubulin III positive cells (*green*) and length measurement of HUCB-NSC cultured on fibronectin (**b**) and poly-L-lysine (**c**) patterns of 10 µm *wide lines*. Cell nuclei are stained with Hoechst (*blue*). Statistically significant difference was observed between the results of the shortest and the longest cells in all experimental groups. *$P < 0.0001$. Adapted and modified from [18]

dated cells longer than 100 µm (Fig. 14a, b). Thus, typical neuronal morphology (longitudinal cells adjusting to the printed lines) was observed only on the fibronectin domains (Fig. 14).

The domains: 120 × 120 µm squares or squares with interconnecting lines immobilized to the surface defined, small population of neural stem cells. We have observed that fibronectin promote cell spreading and neuronal differentiation (presence of neuronal and astrocytic markers—β-tubulin III and S100b, GFAP respectively). Interconnecting 10 µm wide lines enhanced this effect by directing axonal outgrowth (Fig. 15e–h). On the other hand PLL allows for immobilization of non-differentiated, rounded cells (Fig. 15a–d). Addition of dBcAMP further promoted neuronal and astrocytic differentiation in every tested condition.

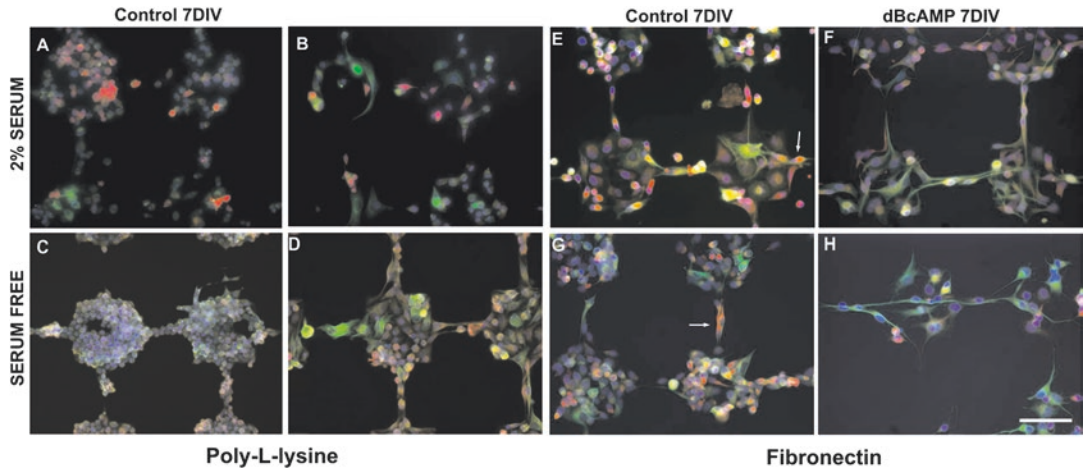

Fig. 15 Immuno-images of HUCB-NSC grown on PLL (**a**–**d**) and fibronectin (**e**–**h**) microarrays for 7 days in serum (**a**, **b**, **e**, **f**) and serum free conditions (**c**, **d**, **g**, **h**) differentiating in the presence of dBcAMP (**b**, **f**, **d**, **h**) or growing as a control cultures (**a**, **c**, **e**, **g**). Neuronal marker β-tubulin III is shown *green* for all images. Astrocytic markers are stained *red* for S100β (**a**–**d**) and GFAP (**e**–**h**). Cells co-expressing GFAP and β-tubulin III reveal an *orange color* (**e**, **g**, *arrows*). Cell nuclei are contra-stained with Hoechst (*blue*). The scale bar is 100 μm for all images. Adapted from [26]

3.5 Neural Stem Cell Fate Control on Microspotted Domains

3.5.1 Characterization of Microspotted Domains

Microarray layouts of different content of biomolecules were prepared to control neural stem cell differentiation. As it was mentioned previously, we have chosen the fibronectin as optimal protein and 84 μg/mL as best concentration in terms of cell adhesion and quality of samples during the entire cell culturing procedure (cell seeding, medium changing, fixation) and data collection (staining and immunofluorescence). We were interested whether signaling molecules, such as CNTF, Notch, Jagged, Wnt3a, Shh, Dkk-1, and BMP4, which all play important roles in the development of the nervous system, can determine the HUCB-NSCs fate. Such data represent important information for the possible functionalization of the biomimetic in vitro cues for controlling cellular differentiation [26].

For that purpose, the solution of fibronectin with concentration 84 μg/mL was used as a control spot, and the signaling molecules, such as CNTF, Notch, Jagged, Wnt3a, Shh, Dkk-1 and BMP4 (R&D Systems) were diluted in fibronectin containing spotting buffer and dropped as an array of spots containing different concentrations of each protein representing different signaling molecules (2.5, 5, and 10 μg/mL) on one glass slide.

Verification of Quality of Microspotted Experimental Domains by Ellipsometry

To test the stability of microspotted array during the washing procedure, after preparing the microspotting on the PEO-like coated silicon slide, we have incubated the samples in PBS for 1 h in incubator. After rinsing in water and drying under nitrogen flow the arrays were tested by the ellipsometry. The results are shown as the thickness maps of deposited fibronectin, signaling molecules in

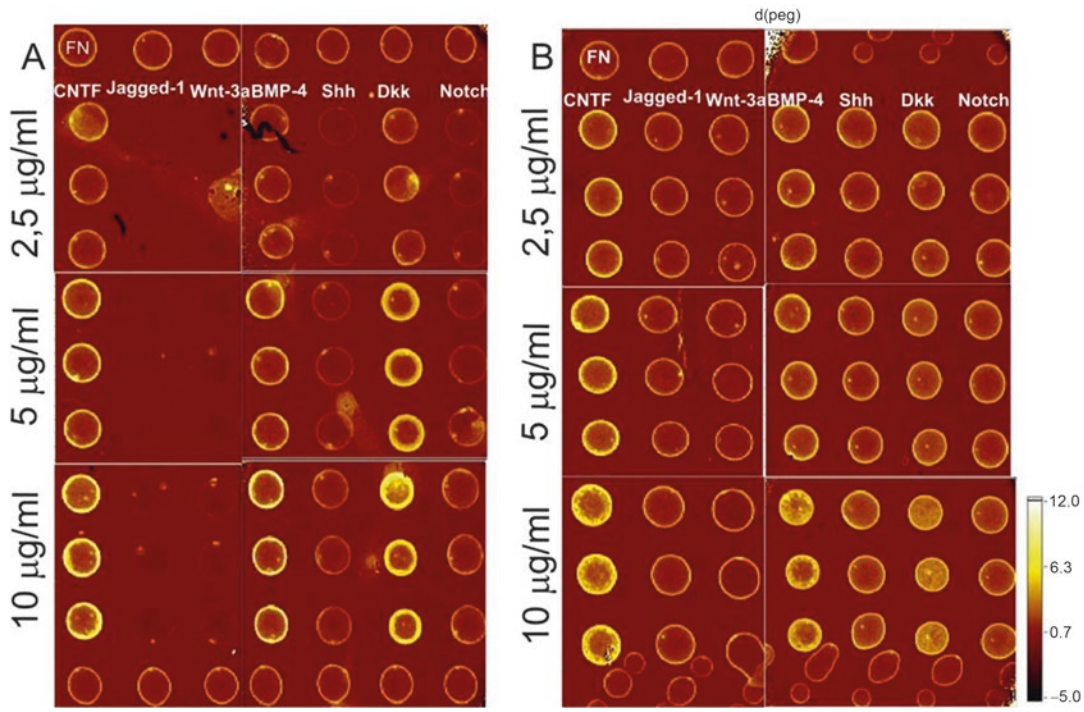

Fig. 16 Thickness map of fibronectin and signaling molecules spotted on plasma-deposited PEO-like film on silicone substrate after rinsing in PBS and measured from ellipsometric Δ and ψ map. The tickness is given in nm with respect to PEO-like deposited on Si master. Signaling molecules spotted alone in printing buffer (**A**), signaling molecules spotted together with fibronectin in printing buffer (**B**)

different concentration and signaling molecules at different concentration mixed with fibronectin solution in printing buffer.

The ellipsometry results showed that after PBS washing in control domains (fibronectin in 84 µg/mL, Fig. 16b, the upper and lower rows) there is a certain amount of the protein that ensures the adhesion of cells to the domains. The control spots containing only the signaling proteins in printing buffer, but lacking the fibronectin (Fig. 16a), were found to contain a certain amount of signaling proteins deposited within the domains (not detected for Jagged-1 and Wnt-3a proteins). However this amount and content was not sufficient for cell adhesion. Fibronectin, which was added to the spotting solution with the SM guarantee the cell resistance and diminish the "ring effect" that is a very common phenomenon in spotting experiments, thus ensuring more uniform protein distribution (Fig. 16b).

Verification of Functionality of Microspotted Experimental Domains by SPR

Several features of bioactive domains have to be considered—the real presence of investigated proteins, e.g., signaling molecules in the domains, the availability of amino acid sequence that is responsible for integrin receptor binding to the extracellular matrix protein and the accessibility of these proteins to the cells' receptors or

ligands. For instance, improper protein folding would not allow for the cell responsiveness. The functional analysis—the biological activity was performed using surface plasmon resonance (SPR) imaging in a GenOptics (France) equipment. Monochromatic laser source of λ = 810 nm measured the changes in the refractive index between gold prism and the dielectric surface). The bioactivity of tested domains was performed on the gold prism surface covered with PEO-like film and deposited with array of spotted fibronectin and fibronectin + SM, using adsorption of antibodies that detect sequence of the deposited biofunctional domains' proteins in respect to the PBS flow, as a reference. To test whether the fibronectin and signaling molecules are within the domains and are biologically active we have used the flow of antibody against the RGD sequence of fibronectin (Ab-RGD), that is necessary for the binding by integrin receptors on the cell surface (Fig. 17) or antibodies specific for individual SM that were spotted with or without fibronectin in printing buffer (Fig. 18). The negative control was performed by flow of bovine serum albumin (BSA). The kinetic curves obtained during measurement by SPR showed adsorption of proteins over time and was detected from each spots/domains that individually react with the antibody (Fig. 17a). The final results expressed as ΔR (%) is the reflectivity difference between measured sample and the baseline (recorded firstly for PBS flow) (Fig. 17b).

We have shown that the amount of the Ab-RGD bounded to the FN domains with signaling molecules is lower than in samples/domains consisting of fibronectin alone (Fig. 17b). This result indicates that the addition of signaling molecules to the printing buffer mixed with fibronectin cause covering/masking of the RGD sequence by the experimental proteins.

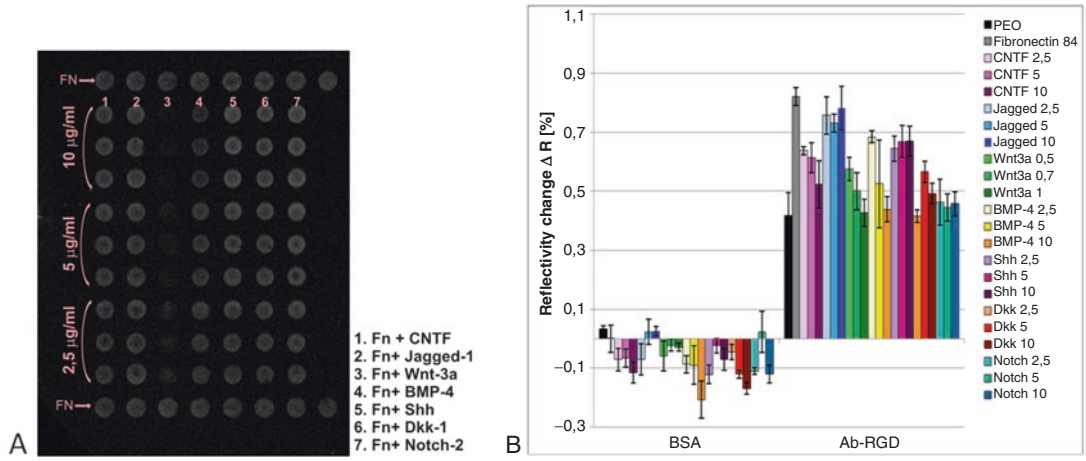

Fig. 17 SPR difference image of the fibronectin (first and last row of the array) and signaling molecules domains after interaction with antibody recognizing the RGD sequence of fibronectin (**a**). The reflectivity difference due to injection of 200 μg/mL BSA, and 10 μg/mL mouse anti-fibronectin RGD-specific antibody (Ab-RGD) measured on spots deposited with different concentration of each signaling molecules (2.5, 5, 10 μg/mL) (**b**)

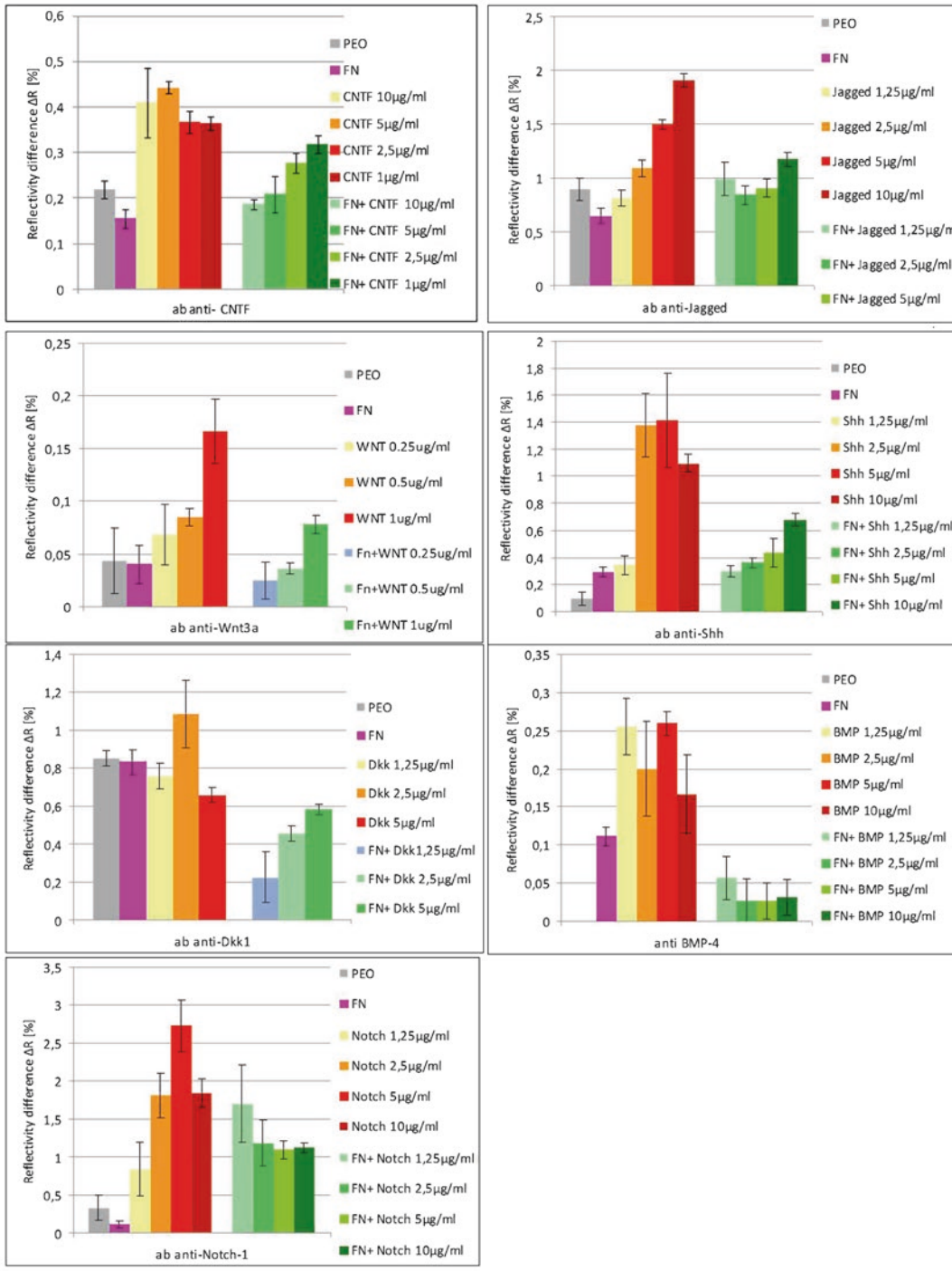

Fig. 18 The reflectivity difference [ΔR (%)] measured on arrays of each SM spotted alone in different concentration and in solution of signaling molecules with fibronectin (FN)

In order to determine the availability of deposited SM for cells, we checked whether the proteins after 2 h of incubation and washing with PBS are still within the domains and accessible for cell receptors or ligands. We measured the adsorption of antibodies specific for every SM on the arrays separate for each SM. These experiments were performed after the BSA treatment of measured domains in order to block unspecific binding of antibody to the spotted proteins, after these washing the flow of specific antibodies were carried out and the reflectivity change was performed (Fig. 18). These experiments showed that the investigated proteins are present within the spots although the fibronectin, that is present in the printing buffer/as a carrier and ECM component slightly masks the selected proteins (Dkk1, BMP4), at least the sites detected by specific to SM antibodies.

Verification of Adhesion of NSC to the Microspotted Domains

Firstly, we wanted to test whether spotting of signaling molecules (SM) alone in printing buffer ensure the cell adhesion. To test this, we spotted arrays of different SM concentration and fibronectin alone as a control. After 5 days of culture we did not observe stable cell adhesion to the domains microspotted only with SM, while the control domains were evenly occupied by neural stem cells (Fig. 19).

We concluded that the carrier protein is necessary for the proper cell adherence to the domains and in the further experiments we diluted the SM in the fibronectin solution.

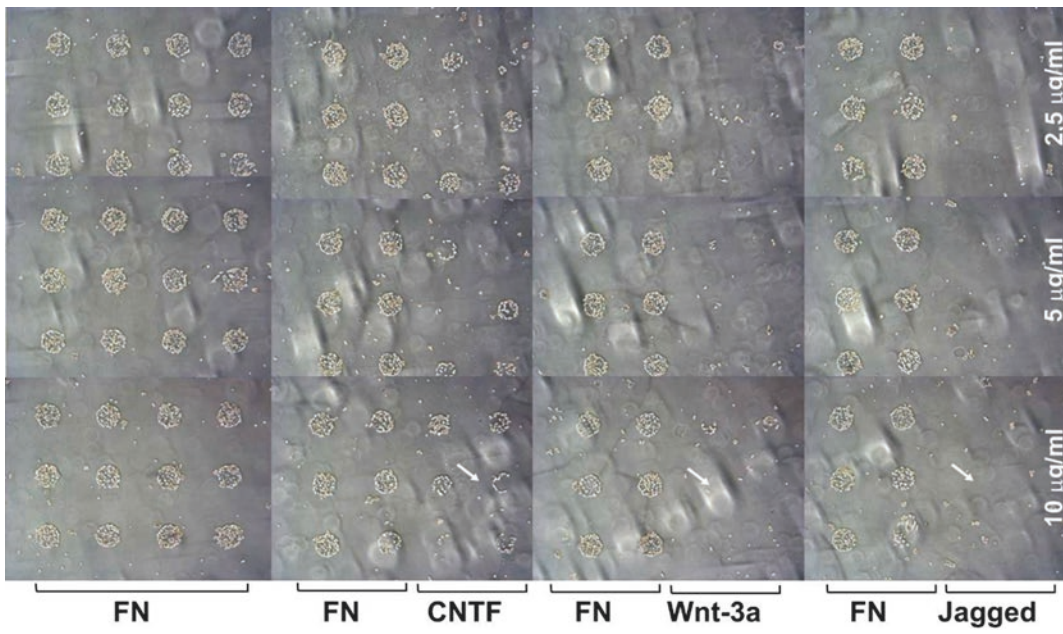

Fig. 19 Optical microscopy of cells seeded on the arrays of microspotted fibronectin domains (FN) or signaling molecules (CNTF, Wnt3a, Jagged) in different protein concentration (2.5; 5 and 10 μg/mL). Note the lack of immobilized HUCB-NSCs to the domains spotted with only the signaling molecules (*arrows*)

3.5.2 Differentiation of NSC on the Biofunctional Domains Microspotted with Signaling Molecules

The structural and functional analysis of biofunctional domains containing signaling molecules were performed for three different concentrations of experimental proteins The presence of signaling molecules was detected even in the domains with the lowest protein concentration (2.5 μg/mL). However, for the investigation of direct of cell differentiation we decided to analyze the highest SM concentration (10 μg/mL) as a variant of the strongest effect.

In order to measure the degree of HUCB-NSC differentiation on the domains we have performed the immunofluorescence of β -tubulin III (as a neuronal) and GFAP (as astrocytic) markers on cells after 4 days of culture. The cells grown on fibronectin spots were used as a reference, since they did not express advanced neuronal and astrocytic markers, remaining non-differentiated. Based on immunocytochemistry analysis we have identified four groups of cells: undifferentiated, that were negative for investigated markers, astrocytes, that expressed GFAP, neurons, that expressed β -tubulin III and cells that co-expressed these markers (transitional phenotype) (Fig. 20). Fibronectin-spotted domains were characterized as reference because of even distribution of certain phenotypes, without statistical significant differences between them. The most potent and statistically significant astrocytic differentiation of HUCB-NSCs was identified on domains comprising: CNTF (33.95% GFAP positive cells), Jagged-1 (31.46%), Notch (33.37%, $p < 0.001$). The lowest percentage of GFAP positive cells was observed on the domains with Wnt-3a (13.81%). The most potent and statistically significant neuronal differentiation, with the highest percentage of β -tubulin III positive cells was demonstrated on spots having Shh protein (37.01%), Dkk-1 (35.22%), Wnt-3a (32.63%) and BMP-4 (32.59%), while the lowest level of neuronal differentiation was detected in the presence of CNTF (21.13%). The astro-neuronal (transitional) phenotype of cells was evenly distributed in every investigated variant. Cells that were negative for both markers were detected on all of tested bioactive surfaces; however, we have observed the highest percentage of GFAP/β -tubulin III negative cells on Wnt-3a spots (35.32%). A statistically significant difference in the number of cells expressing astrocytic marker (GFAP) was found in the domains containing CNTF, Notch and Jagged, while the neuronal marker was predominantly observed on the spots plotted with Dkk-1, Wnt3a and BMP-4. Meanwhile, Wnt3a and SHH remained in the nondifferentiating and self-renewing stage. Such data represent important information for the possible functionalization of the biomimetic in vitro cues for controlling cellular differentiation.

4 Conclusions

This study shows that patterning of adhesion molecules by microcontact printing or piezoelectric spotting, allows for attachment and differentiation of NSCs and can be used to direct their fate.

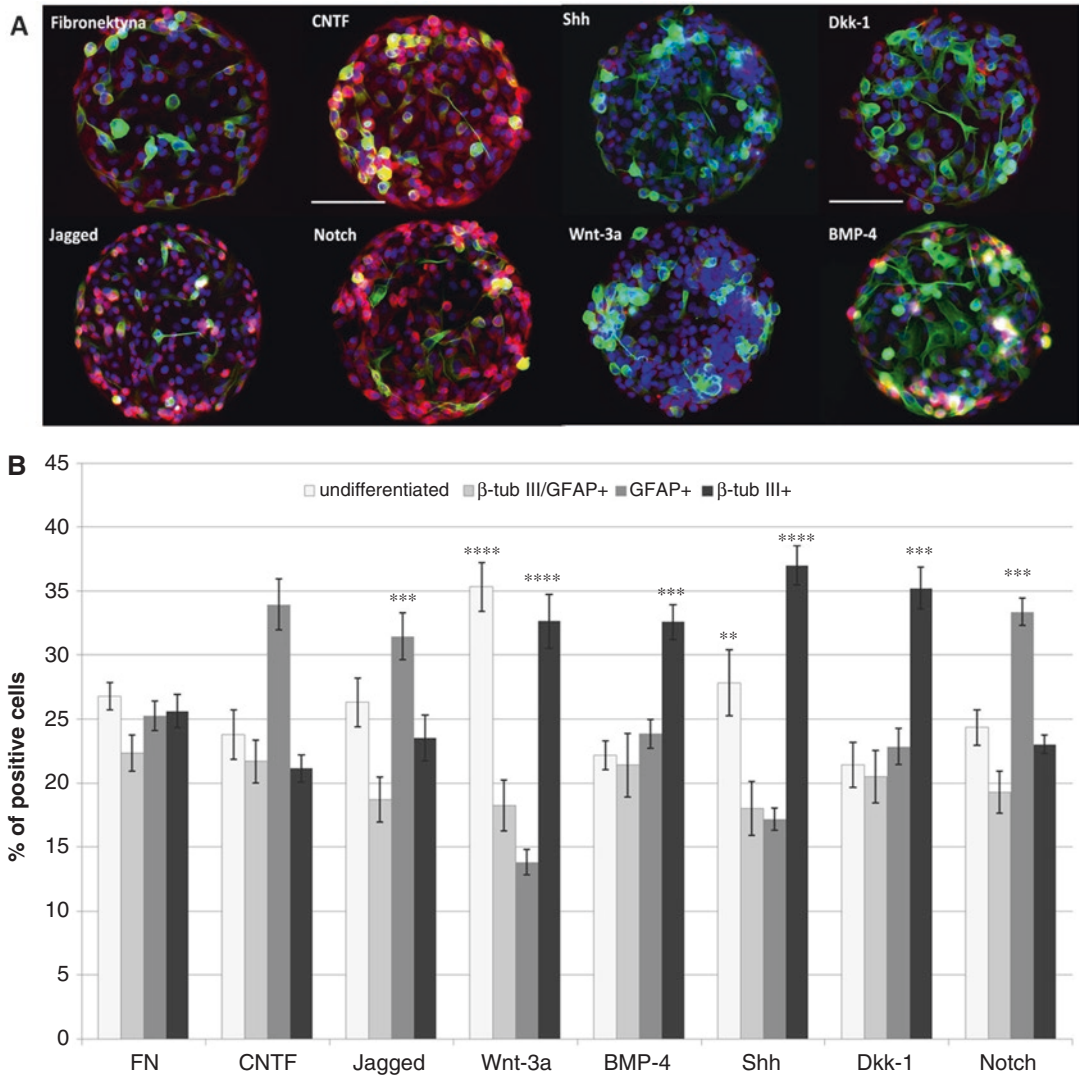

Fig. 20 (**a**) Immunofluorescence imaging of HUCB-NSCs cultured on domains microspotted with different signaling molecules, and stained for β -tubulin III (*green*) and GFAP (*red*) antibodies. Cell nuclei are contra stained with Hoechst 33258 (*blue*). Scale bar = 100 μm. (**b**) HUCB-NSCs differentiation on tested arrays. The phenotype distribution is present as mean % (±SEM) of positive cells for investigated markers. The statistical significant difference is measured in relation to % of positive cells cultured on fibronectin, calculated from five independent experiments (One-Way ANOVA with post hoc Dunnett test, $^{***}p < 0.001$, $^{**}p < 0.01$)

Biofunctional domains with the properties for nonspecific, electrostatic cell membrane–surface interaction (PLL based) versus receptor mediated specific interaction (ECM based) were designed and fabricated with different content of biomolecules and geometry. The ellipsometry and SPR measurements revealed that deposited molecules in bioactive domains are present and functional. They allow for the immobilization of the non-differentiated and highly proliferating population of neural stem/progenitor cells to the

biofunctionalized surface or directional differentiation into neuronal lineage and guiding of the axonal outgrowth. The single cell patterning system (posts and lines) confirmed the influence of pattern geometry on the mode of neural stem cell differentiation. Functional spotted domains were further engineered to create "smart" microenvironment by immobilizing to the surface small signaling molecules together with ECM proteins. Stimulation of selected intracellular pathways by signaling molecules: Wnt, Shh, CNTF, Jagged, Notch, or BMP-4 type resulted in different fate decisions of HUCB-NSC. Wnt-3 and Shh support proliferation and self-renewal, but also neuronal commitment of HUCB-NSCs. Jagged as the ligand and stimulator of Notch signaling pathway and CNTF acting through JAK/STAT directed HUCB-NSC into astrocytic lineage, while Dkk1 and BMP-4 have supported neuronal differentiation. This type of bioengineered cell growth platforms allow for screening the mechanisms governing neural stem cell fate decisions and adverse reactions upon environmental stimuli.

Acknowledgments

We are grateful to Dr Laura Ceriotti for the participation in the microspotting project. We also thank Sabrina Gioria, Patricia Lisboa, G. Ceccone, and Hubert Rauscher for their scientific and technical assistance. This work was supported by statutory founds to MMRC and by Polish Ministry of Scientific Research and Higher Education grant No: 2211/B/P01/2010/38 and European Commission Joint Research Centre Actions "NanoBiotechnology for Health" and "Validation for Consumer Products."

References

1. Lutolf MP, Gilbert PM, Blau HM (2009) Designing materials to direct stem-cell fate. Nature 462(7272):433–441
2. Stabenfeldt SE, Munglani G, García AJ, LaPlaca MC (2010) Biomimetic microenvironment modulates neural stem cell survival, migration, and differentiation. Tissue Eng Part A 16(12):3747–3758
3. Riquelme PA, Drapeau E, Doetsch F (2008) Brain micro-ecologies: neural stem cell niches in the adult mammalian brain. Philos Trans R Soc Lond B Biol Sci 363(1489):123–137
4. Lee MR, Kwon KW, Jung H, Kim HN, Suh KY, Kim K, Kim KS (2010) Direct differentiation of human embryonic stem cells into selective neurons on nanoscale ridge/groove pattern arrays. Biomaterials 31(15):4360–4366
5. Vecino E, Heller JP, Veiga-Crespo P, Martin KR, Fawcett JW (2015) Influence of extracellular matrix components on the expression of integrins and regeneration of adult retinal ganglion cells. PLoS One 10(5):e0125250
6. Kazanis I, Lathia JD, Vadakkan TJ, Raborn E, Wan R, Mughal MR, Eckley DM, Sasaki T, Patton B, Mattson MP, Hirschi KK, Dickinson ME, ffrench-Constant C (2010) Quiescence and activation of stem and precursor cell populations in the subependymal zone of the mammalian brain are associated with distinct cellular and extracellular matrix signals. J Neurosci 21:9771–9781
7. Ruiz A, Buzanska L, Gilliland D, Rauscher H, Sirghi L, Sobanski T, Zychowicz M, Ceriotti L, Bretagnol F, Coecke S, Colpo P, Rossi F (2008) Micro-stamped surfaces for the patterned growth of neural stem cells. Biomaterials 29(36):4766–4774
8. Bużańska L, Zychowicz M, Ruiz A, Ceriotti L, Coecke S, Rausher H, Sobanski T, Wheland M,

Domanska-Janik K, Colpo P, Rossi F (2010) Neural stem cells from human cord blood on bioengineered surfaces—novel approach to multiparameter bio-tests. Toxicology 270:35–42

9. Zychowicz M, Mehn D, Ana Ruiz A, Colpo P, Francois Rossi F, Frontczak-Baniewicz M, Domanska-Janik K, Buzanska L (2011) Proliferation capacity of cord blood derived neural stem cell line on different micro-scale biofunctional domains. Acta Neurobiol Exp (Wars) 71(1):12–23
10. Béduer A, Vieu C, Arnauduc F, Sol JC, Loubinoux I, Vaysse L (2012) Engineering of adult human neural stem cells differentiation through surface micropatterning. Biomaterials 33(2):504–514
11. Joo S, Kim JY, Lee E, Hong N, Sun W, Nam Y (2015) Effects of ECM protein micropatterns on the migration and differentiation of adult neural stem cells. Sci Rep 5:13043
12. Saha K, Pollock JF, Schaffer DV, Healy KE (2007) Designing synthetic materials to control stem cell phenotype. Curr Opin Chem Biol 11(4):381–387
13. Bakhru S, Nain AS, Highley C, Wang J, Campbell P, Amon C, Zappe S (2011) Direct and cell signaling-based, geometry-induced neuronal differentiation of neural stem cells. Integr Biol (Camb) 3(12):1207–1214
14. Dertinger SK, Jiang X, Li Z, Murthy VN, Whitesides GM (2002) Gradients of substrate-bound laminin orient axonal specification of neurons. Proc Natl Acad Sci USA 99(20):12542–12547
15. Millet LJ, Stewart ME, Nuzzo RG, Gillette MU (2010) Guiding neuron development with planar surface gradients of substrate cues deposited using microfluidic devices. Lab Chip 10(12):1525–1535
16. Dalby MJ, Andar A, Nag A, Affrossman S, Tare R, McFarlane S, Oreffo RO (2008) Genomic expression of mesenchymal stem cells to altered nanoscale topographies. J R Soc Interface 5(26):1055–1065
17. Kim WR, Jang MJ, Joo S, Sun W, Nam Y (2014) Surface-printed microdot array chips for the quantification of axonal collateral branching of a single neuron in vitro. Lab Chip 14(4):799–805
18. Zychowicz M, Mehn D, Ruiz A, Frontczak-Baniewicz M, Rossi F, Buzanska L (2012) Patterning of human cord blood-derived stem cells on single cell posts and lines: implications for neural commitment. Acta Neurobiol Exp (Wars) 72(4):325–336
19. Soen Y, Mori A, Palmer TD, Brown PO (2006) Exploring the regulation of human neural precursor cell differentiation using arrays of signaling microenvironments. Mol Syst Biol 2:37
20. Bużańska L, Jurga M, Stachowiak EK, Stachowiak MK, Domanska-Janik K (2006) Neural stem-like cell line derived from a non-hematopoietic population of human umbilical cord blood. Stem Cells Dev 15:391–406
21. Ruiz A, Zychowicz M, Ceriotti L, Mehn D, Sirghi L, Rauscher H, Mannelli I, Colpo P, Buzanska L, Rossi F (2013) Microcontact printing and microspotting as methods for direct protein patterning on plasma deposited polyethylene oxide: application to stem cell patterning. Biomed Microdevices 15(3):495–507
22. Brétagnol F, Lejeune M, Papadopoulou-Bouraoui A, Hasiwa M, Rauscher H, Ceccone G, Colpo P, Rossi F (2006) Fouling and non-fouling surfaces produced by plasma polymerization of ethylene oxide monomer. Acta Biomater 2(2):165–172
23. Bretagnol F, Ceriotti L, Lejeune M, Papadopoulou A, Hasiwa M, Gilliland D, Ceccone G, Colpo P, Rossi F (2006) Functional micropatterned surfaces by combination of plasma polymerization and lift-off processes. Plasma Process Polym 3(1):30–38
24. Ruiz A, Ceriotti L, Buzanska L, Hasiwa M, Bretagnol F, Ceccone G, Gilliland D, Rauscher H, Coecke S, Colpo P, Rossi F (2007) Controlled micropatterning of biomolecules for cell culturing. Microelectron Eng 84:1733–1736
25. Ceriotti L, Buzanska L, Rausche rH, Mannelli I, Sirghi L, Gilliland D, Hasiwa M, Bretagnol F, Zychowicz M, Ruiz A, Bremer S, Coecke S, Colpo P, Rossi F (2009) Fabrication and characterization of protein arrays for stem cell patterning. Soft Matter 5:1406–1416
26. Buzanska L, Ruiz A, Zychowicz M, Rausher H, Ceriotti L, Rossi F, Colpo P, Domanska-Janik K, Coecke S (2009) Patterned growth and differentiation of human cord blood-derived neural stem cells on bio-functionalized surfaces. Acta Neurobiol Exp (Wars) 69:1–14
27. Guemouri L, Ogier J, Zekhnini Z, Ramsden JJ (2000) The architecture of fibronectin at surfaces. J Chem Phys 113:8183
28. Ruiz A, Zychowicz M, Buzanska L, Mehn D, Mills CA, Martinez E, Coecke S, Samitier J, Colpo P, Rossi F (2009) Single stem cell positioning on polylysine and fibronectin microarrays. Micro Nanosyst 1:50–56
29. Margadant C, van Opstal A, Boonstra J (2007) Focal adhesion signaling and actin stress fibers are dispensable for progression through the ongoing cell cycle. J Cell Sci 120:66–76

http://www.springer.com/978-1-4939-7022-3

Stem Cell Technologies in Neuroscience

Srivastava, A.K.; Snyder, E.Y.; Teng, Y.D. (Eds.)

2017, XIV, 240 p. 55 illus., 46 illus. in color., Hardcover
ISBN: 978-1-4939-7022-3
A product of Humana Press